Catalysis Today 175 (2011) 370–379

Contents lists available at ScienceDirect

Catalysis Today

journal homepage: www.elsevier.com/locate/cattod

Catalytic activity and characterization of Pt/calcined CuZnAl hydrotalcites in nitrate reduction reaction in water

A. Aristizábal[a], M. Kolafa[a], S. Contreras[a,*], M. Domínguez[c], J. Llorca[c], N. Barrabés[b], D. Tichit[b], F. Medina[a]

[a] Departament d'Enginyeria Quimica, Universitat Rovira i Virgili, Campus Sescelades, Av.Països Catalans 26, 43007 Tarragona, Spain
[b] Institut Charles Gerhardt UMR 5253 CNRS/UM2/ENSCM/UM1, Matériaux Avancés pour la Catalyse et la Santé, 8 rue Ecole Normale, 34296 Montpellier Cedex 5, France
[c] Institut de Tècniques Energètiques and Centre for Research in NanoEngineering, Universitat Politècnica de Catalunya, Diagonal 647, 08028, Barcelona, Spain

ARTICLE INFO

Article history:
Received 15 October 2010
Received in revised form 15 February 2011
Accepted 28 February 2011
Available online 31 March 2011

Keywords:
Nitrate removal
Catalytic reduction
Cu-Pt
Hydrotalcites
CuZnAl

ABSTRACT

Groundwater pollution with high nitrate concentration has become an important environmental and health issue. Catalytic reduction of nitrates emerged as a promising technique to remove nitrate in water. In the present study, Pt supported on CuZnAl calcined hydrotalcite catalysts with different Cu/Zn ratios (0.5, 1 and 2) were tested in a continuous reactor for the catalytic reduction of nitrates. These materials were characterized by different techniques such as: BET, TPR, XRD, HRTEM, XPS, FTIR. According to the results, the Cu/Zn atomic ratio in the active support has a strong influence in the nitrate conversion and in the nitrogen selectivity, indicating that the interaction of copper in the support plays an important role. The highest nitrogen yield is achieved with a Cu/Zn ratio 1. Also, the incidence of the Pt metal loading was studied in the range of 0.5–2%. This variable does not present a significant influence in the catalytic activity compared to the Cu/Zn ratio, within the range studied. Furthermore, catalysts are stable for this reaction.

1. Introduction

Groundwater pollution with high nitrate concentration has become an environmental and health issue worldwide. The use of fertilizers in agriculture, chemical products and septic tank systems are the main sources of nitrates in water [1]. Nitrate is a potential human health hazard, and subsequently drinking water standards were established to prevent health problems, like clinical cyanosis [2,3].

Different techniques to remove nitrate from water have received increasing attention [4–6]. The research has mainly focused on: catalytic denitrification [7,8], reverse osmosis [9], ion-exchange [10] and biological treatment [11,12]. Catalytic denitrification is one of the most promising techniques for nitrate removal from an ecological point of view, because it transforms nitrates into nitrogen without waste generation [13]. This technique was first described by Vorlop and Tacke [14]. It consists in the nitrate reduction over a bimetallic catalyst using a reducing agent like hydrogen [15]. Its main drawback is the possible formation of ammonia and nitrite, as side products, which are undesirable in drinking water.

Recent studies of the catalytic denitrification technique have been focused on the optimization of the activity and selectivity toward nitrogen formation; studying the incidence of different processes variables (such as: reactor type [16,17], type of reductant [13,18], and pH [19,20]), as well as the influence of different catalysts design variables (like: synthesis method [21–23], kind of support [24–26], and bimetallic pair [27]). Within the studied variables, the nature of the support [24,28,29] has shown to be a defining parameter that affects nitrogen selectivity. Different supports have been used for this reaction like: activated carbon [30,31], CeO_2 [7], Al_2O_3 [27,32], TiO_2 [33,34], resins [35] and calcined hydrotalcite-type materials [20,29,36–38]. Hydrotalcites (HT) are layered double hydroxides that can be represented by the general formula: $[M(II)_{1-x}M(III)_x(OH)_2]^{x+}[(A_{x/n}{}^{n-})]\cdot mH_2O$, where x is typically between 0.25 and 0.33, and A^{n-} is a n-valent interlayer anion. These compounds present positively charged brucite-like layers, $Mg(OH)_2$, with trivalent cations M(III) substituting divalent cations M(II) in octahedral sites of the hydroxides. A wide range of derivatives containing various combinations of M(II), M(III) and A^{n-} ions can be synthesized. Upon calcination, they form homogeneous mixed metal oxides with very small crystal size, which are stable against thermal treatments, and by reduction a high dispersion of the metallic crystallites is obtained. The mixed oxides recover their initial structure when rehydrated; this is called "memory effect" [39].

* Corresponding author. Tel.: +34 977559680; fax: +34 977559621.
E-mail address: sandra.contreras@urv.cat (S. Contreras).

0920-5861/$ – see front matter © 2011 Elsevier B.V. All rights reserved.
doi:10.1016/j.cattod.2011.02.044

The calcined HT based materials used by other authors as catalyst supports for the hydrogenation of nitrates in water include: Pd-Cu/MgAl [20,26,28,37], Pd/CuMgAl [28,29], Pd and Cu co-precipitated in MgAl HT structure [37] and Pd-Sn/MgAl [36], to the best of our knowledge. It was found that during the reaction the HT structure is regenerated, and in this process diffusion limitations affecting the kinetics and the selectivity of the reaction [16,17,29,40] are diminished. The "memory effect" of the HT phase was related to the catalytic behavior of Pd-Cu/MgAl and Pd/CuMgAl catalysts by Palomares et al. [28,29]. Afterwards, Wang et al. [26] reported that Pd-Cu/MgAl calcined HT possessed effective adsorptive and catalytic capacity for this reaction, compared to Al_2O_3, TiO_2 and HZSM supports [20]. Also, Wang et al. [37] compared the catalytic activity of impregnated Pd-Cu/MgAl calcined HT catalysts with different Mg/Al ratios (2,3,4 and 5) to a Pd/CuMgAl catalyst (with copper co-precipitated in the HT structure). Pd/CuMgAl catalyst showed the best catalytic properties due to the higher degree of regeneration of the HT structure and the higher copper dispersion compared to MgAl mixed oxide supports. Moreover, the Mg/Al ratio affects the adsorption capacity of the support and when this capacity increased the catalytic activity was enhanced. A consecutive and dynamic adsorption and catalytic hydrogenation process was proposed by the authors. Similarly, Wan et al. [36] reported that the nitrite selectivity and the activity is directly related to the adsorption capacities using Pd-Sn/MgAl catalysts with different Mg/Al ratio.

The mentioned studies were performed in batch reactors and using Pd as noble metal. However, Pt has been successfully used for this reaction [30,31], and good catalytic results were reported in packed bed reactors (PBR) [30].

These previous studies in the catalytic reduction of nitrates that included HT-type materials are focused on MgAl and CuMgAl calcined HTs, materials well known for their basic properties [41]. Moreover, these studies reported high ammonium concentrations [28] that should be decreased. In this way, a previous study demonstrated that the ammonium formation could be effectively controlled by tuning the acid–base properties of the support [7]. One possibility to modify the acid–base properties of CuMgAl calcined HT materials, is to introduce Zn instead of Mg in the HT structure [39,41] in order to increase the acidic character. However, this affects the reconstruction ability that was claimed to be a determinant variable in HT supported catalysts for this reaction. Moreover, CuZnAl calcined HT are active and selective catalysts in several chemical processes including: water gas shift reaction [42], oxidative methanol reforming reactions [43], oxidative steam reforming of methanol [44], etc. For these reactions, the catalytic performance is strongly influenced by the chemical composition of the CuZnAl mixed oxides.

From literature reports, it seems that the use of CuZnAl calcined HTs as supports in the catalytic reduction of nitrates could arise in interesting results. In the present study, Pt supported on CuZnAl calcined HT catalysts are tested in the hydrogenation of nitrates in water, with the aim of studying the influence of the composition of the support on the catalytic activity. The influence of the Cu/Zn atomic ratio (0.5, 1 and 2) in the activity and selectivity for the reaction is discussed on the basis of the microstructure properties of the catalysts, characterized mainly by XRD, XPS, HRTEM and TPR. Moreover, the influence of the Pt metal loading (2, 1 and 0.5 wt%. supported on CuZnAl calcined HT with Cu/Zn ratio 1) is studied, in order to improve nitrogen selectivity [45]. In the investigation, copper is co-precipitated in the HT structure to obtain high dispersion of the active phase. Also, the reactions were performed in a continuous PBR and hydrogen is selected as reducing agent. Additionally, nitrate adsorption tests are carried out to study the effect of the nitrate adsorption in the catalytic activity.

2. Experimental

2.1. Characterization techniques

2.1.1. Atomic absorption spectroscopy

Atomic absorption spectroscopy (HITACHI Z-8200) was used to determine the elemental chemical analysis of Cu, Zn and Al in the HT precursors and the copper concentrations in the treated effluent. For the chemical analysis, 0.5 g of each sample was dissolved in 5 ml of concentrated nitric acid and then diluted to 25 ml with distilled water. The aqueous samples were preserved with concentrated nitric acid.

2.1.2. Thermogravimetric analysis (TGA)

The HT precursors were analyzed by TGA on Netzsch STA 409 PC/4/H Luxx. The analyses were performed under 20 ml/min of synthetic air flow and with a heating rate of 10 °C/min.

2.1.3. Powder X-ray diffraction (XRD)

XRD patterns were measured using a Bruker-AXS D8-Discover diffractometer with parallel incident beam (Gobel mirror) and vertical θ–θ goniometer, a 0.02° receiving slit and scintillation counter as a detector. The angular 2θ diffraction range was between 5° and 70°. The data were collected with an angular step of 0.05° at 3 s per step. CuKα radiation was obtained from a copper X-ray tube operated at 40 kV and 40 mA.

Thermal analysis of the samples, were monitored by XRD using a Siemens D5000 diffractometer (Bragg–Brentano parafocusing geometry and vertical θ–θ goniometer) equipped with an Anton-Paar HTK10 platinum ribbon heating stage. Ni-filtered CuKα radiation (30 mA, 40 kV) and a Braun position sensitive detector (PSD) were used. The angular 2θ diffraction range was between 10 and 60°, step size −0.02° and 0.4 s/step. The patterns were collected from room temperature at $\Delta T = 2$ up to 450 °C with a heating rate of 10 °C/min. A static air-atmosphere was used throughout the measurement.

X-ray patterns were compared to X-ray powder references to confirm phase identities using the Joint Committee on Powder Diffraction Standards (JCPDS, 2006) files.

2.1.4. Surface area measurements

The surface area of the samples were carried out in a Micromeritics ASAP 2010 apparatus, using the BET method from the nitrogen adsorption isotherms at 77 K. Prior to the analysis the samples were degasified 5 h at 120 °C.

2.1.5. Infrared spectroscopy (FT-IR)

FT-IR measurements were carried out in a Jasco FT/IR-600 Plus spectrometer. Background corrections were performed and the spectra were recorded by accumulating 64 scans at a spectral resolution of 2 cm^{-1}.

2.1.6. H_2 temperature-programmed reduction (H_2-TPR)

H_2-TPR analyses were performed in a TPD/R/O 1100 (ThermoFinnigan) equipped with a thermal conductivity detector (TCD). About 50 mg of the samples were placed in a quartz reactor and reduced in a stream of 20 ml/min of H_2 (5 vol% in Ar) at a heating rate of 10 °C/min. The hydrogen consumption due to the reduction of the samples was continuously monitored by the TCD.

2.1.7. X-ray photoelectron spectroscopy (XPS)

XPS spectra were recorded at a pressure below 10^{-9} mbar with a SPECS system equipped with an Al anode XR50 source operating at 150 W and a Phoibos MCD-9 detector (pass energy 25 eV). Prior to the analysis, samples were reduced in situ at 300 °C and atmospheric pressure in a SPECS high pressure cell integrated in

Table 1
Reaction conditions.

Parameter	Value
Mass of catalyst	0.5 g
Hydrogen flow	3 ml/min
Feed	1.2 ml/min
Temperature	25 °C
Pressure	1 atm

the system. Binding energies (accuracy ± 0.1 eV) were referred to the C 1s signal (adventitious carbon).

2.1.8. High Resolution Transmission Electron Microscopy (HRTEM)

HRTEM studies were carried out with a field emission gun microscope JEOL 2010F, which works at 200 kV and has a point-to-point resolution of 0.19 nm. Samples were deposited from alcohol suspensions on standard Cu grids with holey carbon films. Prior to analysis, samples were reduced at 300 °C.

2.2. Sample synthesis

CuZnAl HT with a (Zn + Cu)/Al molar ratio of 3 and different Cu/Zn molar ratios: 2, 1 and 0.5, were prepared by co-precipitation method, at room temperature. An aqueous solution containing $Zn(NO_3)_2{\cdot}6H_2O$, $Al(NO_3)_3{\cdot}9H_2O$ and $Cu(NO_3)_2{\cdot}3H_2O$ in adequate amounts, and a second solution of NaOH (2 M) were slowly and simultaneously added drop by drop to a beaker containing Milli-Q water under vigorous stirring. The pH value was maintained around 10 by NaOH addition. The suspensions were aged under stirring overnight. The resulting solids were filtered and washed several times with Milli-Q water. The light blue or greyish blue colored HT precursors were dried in air at 80 °C for 12 h and grounded in a mortar. The samples were denoted HTCuZnAl-Y, where Y refers to the Cu/Zn atomic ratio.

The HTCuZnAl-Y samples were then calcined at 450 °C overnight to obtain the mixed oxides. The calcined samples were denoted CuZnAl-Y.

The CuZnAl-Y samples were then wet-impregnated with Pt using an aqueous solution of H_2PtCl_6.

2.3. Catalytic activity

The samples were packed in a continuous PBR co-current reactor and then tested as catalysts for the nitrate reduction in water, at atmospheric conditions. The samples were pretreated at 300 °C under hydrogen flow (7 ml/min) for 2 h before the catalytic or adsorption tests. Afterwards, a hydrogen stream and a solution of 100 mg/L of nitrate (Riedhel de Haen, CAS 7631-99-4) in Milli-Q water were fed to the reactor (Table 1 summarizes the reaction conditions). Catalytic tests were performed at least twice to check the reproducibility of the results.

Adsorption tests were performed at the same experimental conditions described for the catalytic tests, except that during these tests no hydrogen was fed to the reactor.

Aqueous samples from the reactions were analyzed by high performance liquid chromatography (HPLC). An anion separation column (Shodex IC SI-90 4E) for suppression method was used to determine nitrate and nitrite concentration, and a Shodex IC YK-421 was used for ammonium determination.

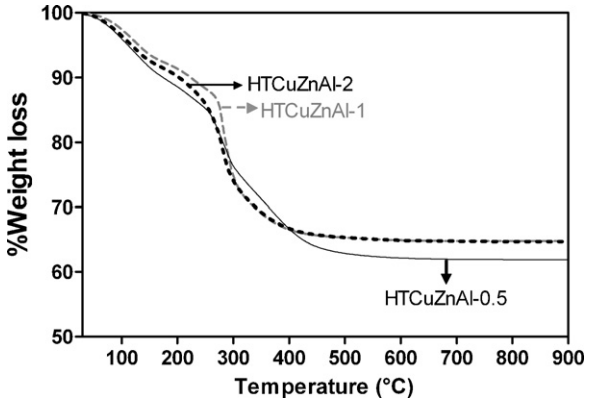

Fig. 1. TGA curves for the thermal decomposition of the hydrotalcite precursors.

3. Results and discussion

3.1. Characterization results

3.1.1. Atomic absorption spectroscopy

The elemental composition of the CuZnAl HT precursors (HTCuZnAl-Y) was determined by atomic absorption. The Cu/Zn, (Cu + Zn)/Al bulk molar ratios experimentally determined were calculated, and are presented besides the theoretical values in Table 2. It is observed that the experimental values are quite similar to the expected values.

3.1.2. Thermogravimetric analysis

Calcination of the HT precursors was followed by TGA measurements. The resulting curves are shown in Fig. 1. The thermal decomposition can be divided into two steps in all cases. First, from 50 to 190 °C the signal indicates the emission of weakly bonded interlayer water molecules. The second weight loss, between 180 and 450 °C, is assigned to the dehydroxylation of the brucite-like layers and the decomposition of the anions located in the interlayer space. All the samples presented similar weight losses around 36 wt% that is typical from HT structure. The samples with Cu/Zn ratio 2 and 1 presented the same total weight loss (34 wt%). When copper content is diminished to 25.3 mol% the final decomposition temperature and the weight loss increased (38 wt%).

3.1.3. Analysis by XRD

Fig. 2 presents the XRD patterns of the HTCuZnAl-Y samples. The patterns showed the characteristic peaks associated to HT phase (JCPDS 01-089-0460). The d_{003} reflection around 0.87 nm

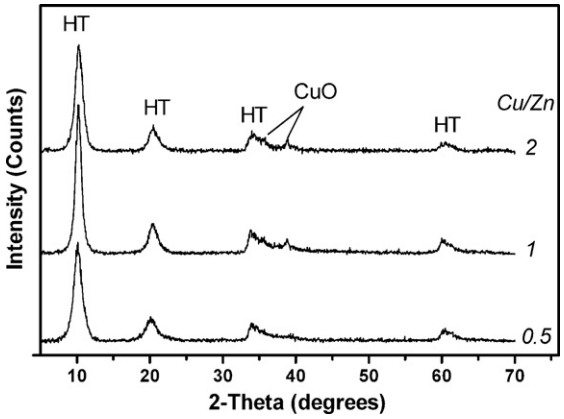

Fig. 2. Power X-ray diffraction patterns of hydrotalcite precursors with different Cu/Zn ratios.

Table 2
Elemental composition, Cu/Zn and (Cu + Zn)/Al molar ratios of the HT precursors.

Hydrotalcite precursors	mol% Cu[a]	mol% Zn[a]	mol% Al[a]	Cu/Zn	(Cu + Zn)/Al
HTCuZnAl-2	49.9 (50)	24.8 (25)	25.3 (25)	2.01 (2)	2.95 (3)
HTCuZnAl-1	38.0 (37.5)	36.4 (37.5)	25.6 (25)	1.04 (1)	2.90 (3)
HTCuZnAl-0.5	25.3 (25)	50.3 (50)	24.4 (25)	0.50 (0.5)	3.0 (3)

Theoretical values are given in parentheses.
[a] Concentrations are normalized to the total metal content.

indicates the presence of nitrates as compensating anions. Tenorite phase at $2\theta = 35.8^\circ$ and 39° (JCPDS 01-1117 file) is also detected in small amount, except for the sample with the lowest Cu/Zn atomic ratio (CuZnAl-0.5). The formation of the tenorite phase could be attributed to: (i) the low Al content and high Cu/Zn atomic ratios (pure CuM(II)M(III) HT compounds are formed for Cu/M(II) ratios ≤ 1 [39,46]); (ii) to the Jahn–Teller distortions introduced by Cu(II) into the brucite-like layers [39,46]; and (iii) to the transformation of $Cu(OH)_2$ into CuO (this fact was evidenced by the change of the color from light blue into a dark color during drying [47]. Moreover, the darkness of the samples increases with the copper content). Furthermore, the presence of other non-crystalline side phases cannot be discarded [39].

The thermal decomposition of the HTCuZnAl-Y samples was monitored by XRD in a diffraction chamber, in order to study the phase evolution of these materials during calcination. Fig. 3 shows the sequence of patterns with increasing temperature. All the patterns in the thermal study present peaks at $2\theta = 39.8^\circ$ and 42.2° corresponding to the platinum support (JCPDS 4-802) used in the analysis. During the calcination, the peaks associated to the HT phase are progressively shifted to higher angles, and decreased in intensity with increasing temperature up to 180 °C. This is due to the decrease in the interlayer distance attributed to the removal of water in the interlayer [47], which agree with the first weight loss in the TGA results (see Fig. 1). With a further increase in temperature, the HT phase totally collapsed by dehydroxylation, and oxide phases start to crystallize at around 260 °C for all the samples.

The CuZnAl-0.5 sample, presents at 260 °C weak reflections of a zincite phase (JCPDS 36-1451, $2\theta = 31.8^\circ$, 34.4°, 36.2°, 47.5° and 56.6°) and a small increase of the intensity of these peaks at higher calcination temperatures is observed (see Fig. 3A). However, the presence of CuO is not observed during this XRD thermal treatment probably due to the low crystallization time during the experiment. In this case the presence of an amorphous CuO phase formation cannot be excluded. On the contrary, CuZnAl-1 sample (Fig. 3B) presents both ZnO and CuO diffractions peaks above 180 °C. CuZnAl-2 (Fig. 3C) presents CuO reflections at 260 °C, but when the calcination temperature increased up to 350 °C the appearance of an incipient ZnO phase is observed. The differences in the diffraction patterns clearly indicate that the nature of the phase evolution is strongly influenced by the Cu/Zn atomic ratio. Moreover, the intensity of the CuO peaks increase with the copper content. Reflection of spinel-type compounds are absent in the XRD pattern in all cases.

Based on the results of the thermal studies, the HT precursors were calcined at 450 °C overnight to obtain the corresponding mixed oxides to be used as catalysts active supports. Fig. 4 presents the XRD patterns of the CuZnAl-Y sample. CuO and ZnO phases appear in the three samples, however the crystallinity of these phases strongly depends on the Cu/Zn atomic ratio. For CuZnAl-0.5 and CuZnAl-1 the main crystalline phase detected is ZnO, while for CuZnAl-2 is CuO. The presence of spinel-type phases is not discarded.

The diffraction patterns of Pt impregnated materials (not shown) are similar to the patterns of CuZnAl-Y samples (Fig. 4). Peaks associated to platinum species are not observed, probably due to the low Pt content (up to 2 wt%.) and good metal dispersion (see Section 3.1.8).

In addition, changes in the XRD patterns of the catalysts are observed after the reduction at 300 °C during 2 h (Fig. 5). In this case, additionally to the CuO and ZnO phases previously mentioned, peaks corresponding to metallic copper (JCPDS 01-070-3038) appeared at 43° and 50.5°. The intensity of this copper phase increases with the amount of copper in the sample at expenses of the CuO phase. Moreover, after the catalytic tests partial reconstruction of the mixed oxide structure is not detected. This fact

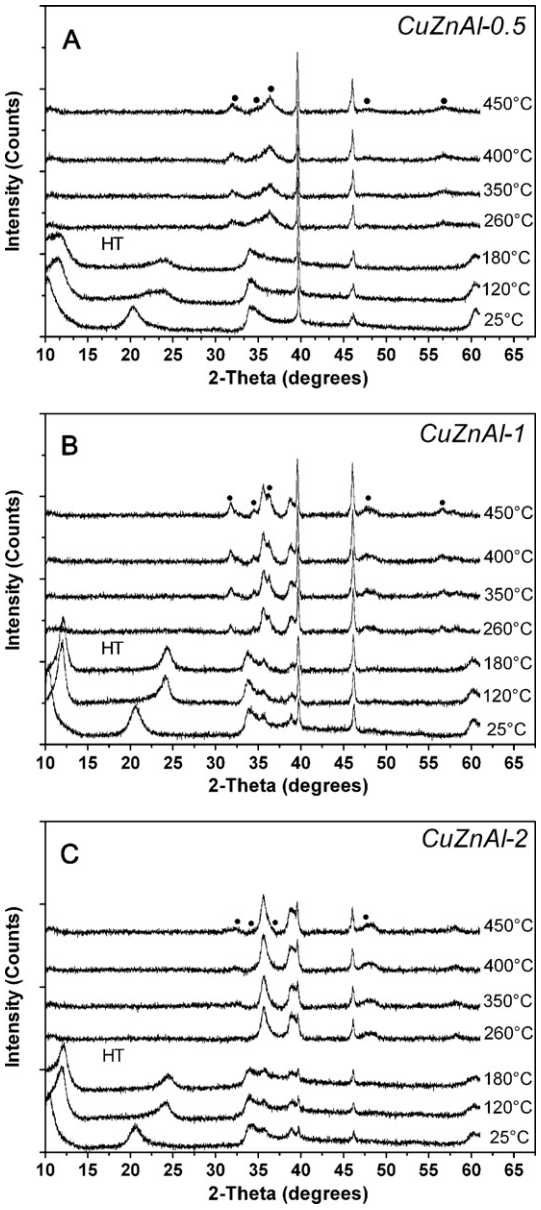

Fig. 3. XRD pattern of hydrotalcite precursor at different calcination temperatures.

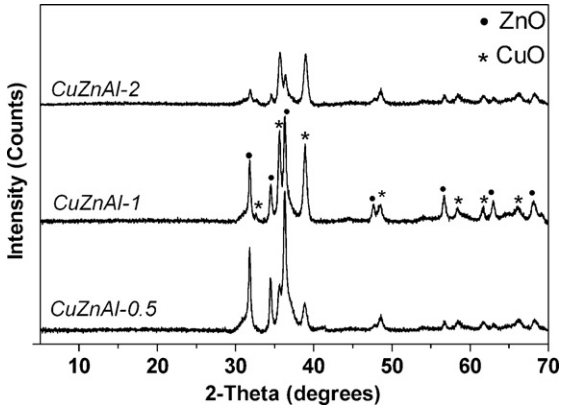

Fig. 4. Power X-ray diffraction patterns of hydrotalcite precursors calcined at 450 °C overnight.

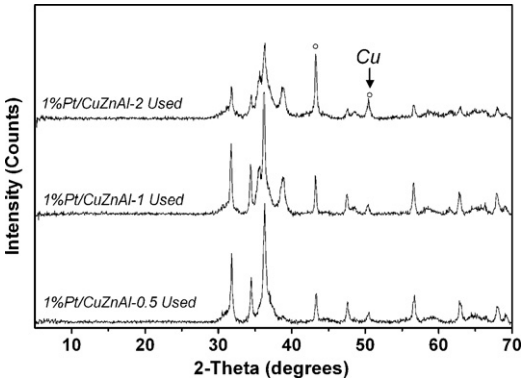

Fig. 5. Power X-ray diffraction patterns of 1%Pt impregnated materials.

indicates that the reconstruction of the CuZnAl mixed oxide phases to HT like structure is not performed during the catalytic process contrarily to the results previously reported for CuMgAl and MgAl samples [29].

3.1.4. Surface area of the samples

The BET surface areas of CuZnAl-Y samples are quite similar, and the values are between 42 and 55 m^2/g (see Table 3). These results are similar to the results reported by Behrens et al. [47] and Breen et al. [48]. A slight increase of the BET surface areas is observed when Pt is impregnated. The increase of the surface area could be explained by the addition of H_2PtCl_6 as platinum precursor. The acid platinum precursor probably produces a partial solution of the solid sample creating more porosity.

3.1.5. Infrared analysis

The samples at the different stages of the study were characterized by FT-IR. Fig. 6 presents the FT-IR results of the HTCuZnAl-Y samples. All samples show similar spectra, subtle differences are noted. The bands recorded at 1636 cm^{-1} and around 3000 to

Table 3
Surface area for calcined samples with different Cu/Zn atomic ratios and Pt impregnated samples.

Sample	BET surface area (m^2/g)
CuZnAl-2	42.0
CuZnAl-1	48.0
CuZnAl-0.5	54.7
1%Pt/CuZnAl-2	51.9
1%Pt/CuZnAl-1	52.8
1%Pt/CuZnAl-0.5	62.9

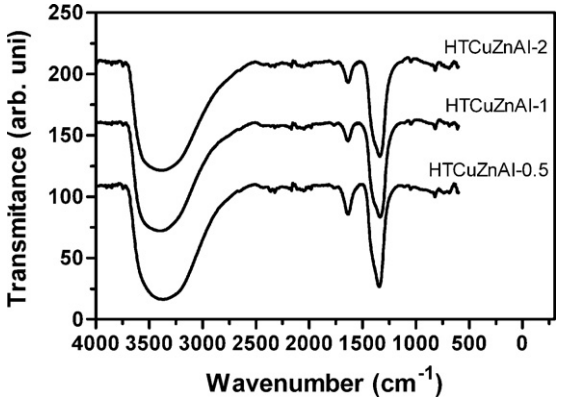

Fig. 6. Infrared spectra of the hydrotalcite precursors.

3700 cm^{-1}, are due to hydroxyl groups of the interlayer water molecules. These bands are broader and more intense when Cu/Zn ratio decreases probably due to the presence of more pure HT phase. The narrow band at 1336 cm^{-1} is assigned to interlayer nitrate anions confirmed by XRD [29].

Fig. 7 presents the FT-IR spectra of CuZnAl-Y samples (450 °C). The band at 1336 cm^{-1} disappears due to the thermal decomposition of nitrate at this temperature, indicating the destruction of the HT like structure. Also, the band at 3000 to 3700 cm^{-1} decreases in intensity due to the water removal (the persistence of this band is probably due to the presence of water moisture during the manipulation of the sample). Furthermore, a narrow peak at 686 cm^{-1} appears due to the transformation of the HT phase into mixed oxides. After contacting the materials with water during the reaction, there is no evidence of the reconstruction of the mixed oxide phases to HT structure.

3.1.6. Reducibility by H_2-TPR

The reduction properties of the samples were examined by H_2-TPR, and the results are shown in Fig. 8. It is observed that the Cu/Zn atomic ratio and the presence of Pt in the samples influence the reduction of the catalysts. In Fig. 8 it can be seen that the CuZnAl-Y samples have similar profiles, consisting of a main reduction peak with a maximum temperature in a range between 278 and 300 °C, according to previous results [48,49]. These peaks could be attributed to the reduction of Cu(II)O species [49,50], detected by XRD. The maximum reduction temperature of these samples increases when the copper content increases, and this could be explained by a poor dispersion of copper and by an increase in the interaction between the copper oxide species and the support [43] when the Cu/Zn ratio increases. Furthermore, CuZnAl-2 sam-

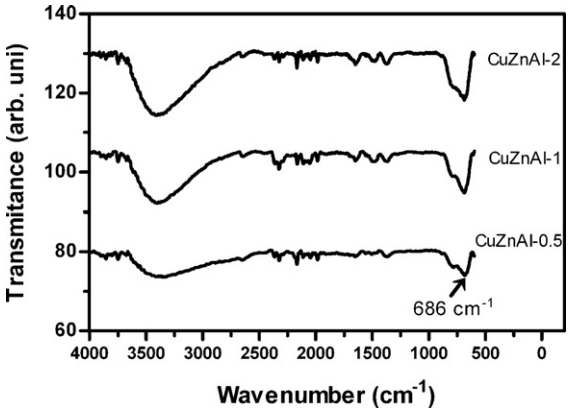

Fig. 7. Infrared spectra of the calcined hydrotalcite precursors at 450 °C over-night.

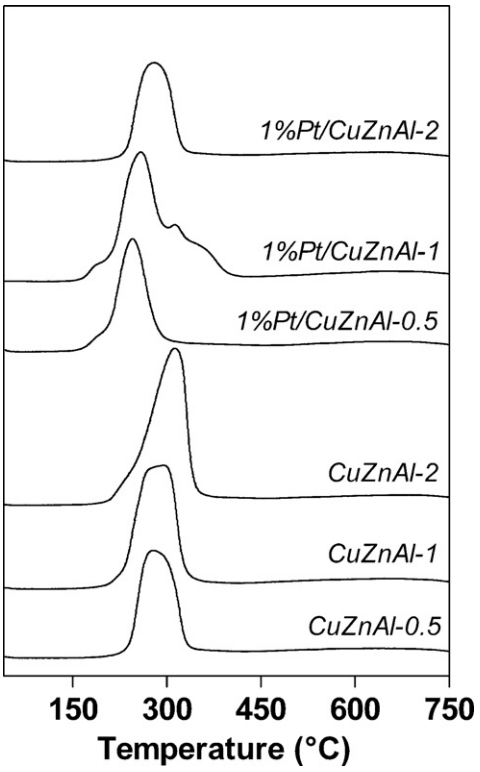

Fig. 8. H_2-TPR profiles of the calcined HT precursors and 1%Pt/CuZnAl catalysts.

ple presents a shoulder at 220 °C that could be due to the reduction of amorphous or to highly dispersed copper oxide [50]. Copper(II) oxide standard (not shown) presents a single peak at higher reduction temperature (364 °C) compared to the samples, indicating that, even considering the high amount of copper, there is a good dispersion of copper in the support (supported CuO reduces more easily than bulk CuO [51]).

The addition of Pt to the CuZnAl-Y samples increases the CuO reducibility; as a result the reduction peaks are shifted to lower temperatures (the maximum reduction temperatures are registered in a range between 237 and 271 °C). These peaks are attributed to copper oxide species that interacts in a different way with Pt and with the support. Samples 1%Pt/CuZnAl-1 and 1%Pt/CuZnAl-0.5 present a shoulder around 177 °C that could be assigned to well dispersed copper oxide in interaction with Pt. Sample 1%Pt/CuZnAl-1 also presents shoulders at 300 and 340 °C that could be attributed to copper species that have no interaction with platinum or is not well dispersed. Sample 1%Pt/CuZnAl-2 has possibly a more homogeneous CuO phase distribution according to the symmetry of the peak. In all cases, hydrogen consumption is mainly due to CuO species, considering that the Pt content is too low compared to the copper content. No reduction peaks for platinum oxide are observed, probably due to the high amount of Cu compared to the Pt one.

For all the samples, peaks at higher reduction temperatures (up to 750 °C) were not observed.

3.1.7. XPS

1%Pt/CuZnAl samples were reduced in situ at 300 °C (at the same conditions described for the catalysts), and then analyzed by XPS in order to determine the chemical state of the metals. In Table 4 the surface atomic composition of the reduced samples with 1 wt% Pt content are compiled. The ratios are calculated from the respective Zn $2p_{3/2}$, Cu $2p_{3/2}$, Al 2s and Pt $4d_{5/2}$ core levels.

Table 4
XPS surface atomic ratios for reduced catalysts with 1 wt% Pt content.

Sample	Zn/Al	Cu/Al	Pt/Al	Cu/Zn	Cu_{Red}/Cu_{Ox}
1%P/CuZnAl-2	1.34	0.51	0.03	0.38	1.66
1%P/CuZnAl-1	1.46	0.54	0.04	0.37	3.42
1%P/CuZnAl-0.5	1.07	0.23	0.03	0.21	6.87

Cu_{Red}/Cu_{Ox}: copper species reduced over oxidized.

In all samples, Pt $4d_{5/2}$ binding energies at 314.2 ± 0.5 eV correspond to Pt metal, whereas Cu $2p_{3/2}$ exhibits always two contributions at 932.5 ± 0.3 and 933.8 ± 0.5 eV, which correspond to reduced and oxidized Cu species, respectively (Table 4). The surface atomic composition of samples 1%Pt/CuZnAl-1 and 1%Pt/CuZnAl-2 are quite similar in spite of the different nominal Cu/Zn ratio of samples (1 and 2, respectively), whereas sample 1%Pt/CuZnAl-0.5 exhibits a lower surface Cu/Zn atomic ratio (as expected since this sample contains a Cu/Zn nominal value of 0.5). In all cases the dispersion of Pt is similar (nominal loading 1% w/w) and the high Pt/Al atomic ratio determined by XPS indicates that Pt is well dispersed (small particles) and exposed on the surface of the catalysts. Concerning Cu species, it is interesting to note that the ratio Cu_{Red}/Cu_{Ox} can be related to the Cu/Zn nominal value of samples. The lower the Cu/Zn nominal value, the higher amount of reduced copper. (Here it is used Co_{Ox} for Cu(II) and Cu_{Red} for Cu(0) + Cu(I) since it is difficult to distinguish them).

3.1.8. HRTEM

Samples with 1%Pt content were analyzed by TEM to determine the size and morphology of the particles in the samples. All samples were reduced at 300 °C prior to TEM analysis. Fig. 9A shows a typical image of sample 1%Pt/CuZnAl-1 at low magnification. The sample is mostly comprised by very small crystallites in the range 3–6 nm. The same appearance was observed for the other two samples, 1%Pt/CuZnAl-0.5 and 1%Pt/CuZnAl-2. A detailed HRTEM analysis confirms the morphology of all three samples as well as the crystalline nature of the particles. All particles are crystalline and no amorphous phases are detected. Fig. 9B shows a representative HRTEM image of sample 1%Pt/CuZnAl-1 along with a ring electron diffraction pattern of the same area (SAED). The indexation of the electron diffraction pattern is included in the figure and shows that the sample is comprised by crystallites of γ-Al_2O_3, ZnO, and a mixture of CuO and Cu (confirmed by XRD). No signals corresponding to Pt-containing phases have been observed in the SAED pattern due to the low Pt loading of the sample. The same crystalline phases have been identified in samples 1%Pt/CuZnAl-1 and 1%Pt/CuZnAl-0.5.

Representative HRTEM images for these samples are depicted in Fig. 10A and B. Concerning platinum, well-dispersed metallic Pt particles of about 1.5–2.0 nm in diameter have been observed mostly on γ-Al_2O_3 and ZnO, and very rarely in contact with CuO or Cu crystallites. In Fig. 10C some Pt particles are indicated by arrows.

Fig. 11A shows a HRTEM image of a Pt particle on γ-Al_2O_3 in sample 1%Pt/CuZnAl-2. Lattice fringes at 2.27 and 4.56 Å correspond to {1 1 1} crystallographic planes of Pt and Al_2O_3, respectively (see inset). Fig. 11B and C shows Pt particles of 1.5–2.0 nm in size on both Al_2O_3 and ZnO in sample 1%Pt/CuZnAl-0.5. A detailed lattice fringe for one of them oriented along the [1 1 0] crystallographic direction is depicted in Fig. 11C along with the corresponding FT image (see inset).

3.2. Catalytic reduction of nitrates

The catalytic activity and the nitrate adsorption capacity of the samples are discussed. Steady state values have been considered to compare the results.

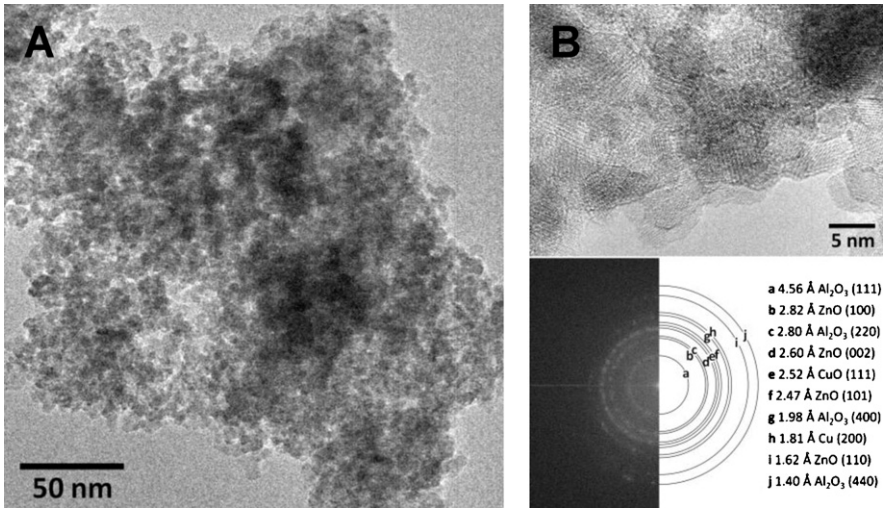

Fig. 9. Sample 1%Pt/CuZnAl-1 (A) Low magnification TEM image, (B) HRTEM image and selected-area electron diffraction pattern with ring identification.

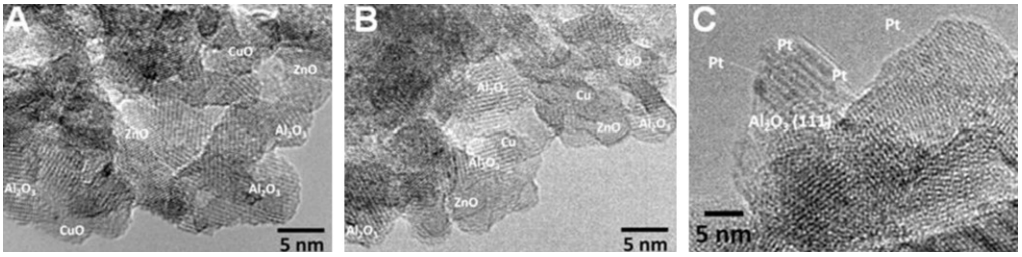

Fig. 10. HRTEM image of: (A) 1%Pt/CuZnAl-2, (B) 1%Pt/CuZnAl-0.5, (C) 1%Pt/CuZnAl-1.

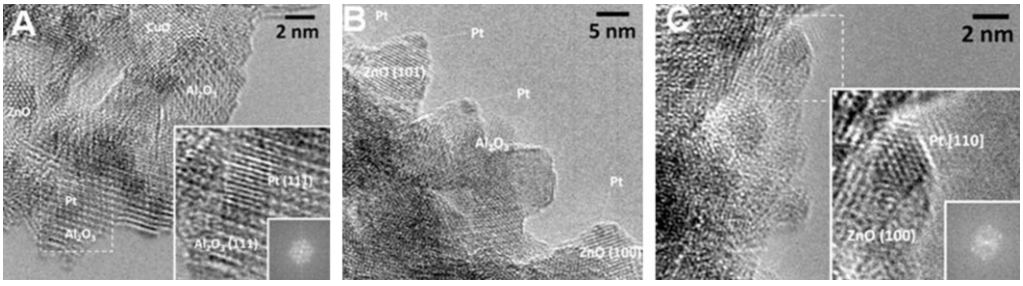

Fig. 11. HRTEM image of sample (A) 1%Pt/CuZnAl-2, (B) 1%Pt/CuZnAl-0.5 and (C) 1%Pt/CuZnAl-0.5. (The enlargement and FT image correspond to the area enclosed in the square).

The conversion, yield and selectivities are calculated according to:

$$X_{\text{Nitrate}} = \frac{C_{\text{initial}}}{C_{\text{initial}} - C_{\text{final}}} \times 100 \quad (1)$$

$$S_{\text{i}} = \frac{\text{moles of i produced/L}}{\text{moles of nitrate converted/L}} \times 100 \quad (2)$$

$$Y_{\text{i}} = \frac{X_{\text{Nitrate}} \times S_{\text{i}}}{100}; \quad Y_{\text{i}} \leq 100 \quad (3)$$

where X_{Nitrate}: nitrate conversion; C_{final}: final concentration of nitrates in the effluent at steady state. C_{initial}: initial concentration of nitrates fed to the reactor (around 100 ppm). S_{i}: selectivity toward product i in steady state. Y_{i}: yield of product i. i: nitrites, nitrogen or ammonium.

3.2.1. Incidence of the Cu/Zn atomic ratio

The catalytic activity of 1%Pt/CuZnAl-Y samples with different Cu/Zn atomic ratios in the hydrogenation of nitrates in water using a continuous reactor is discussed. Fig. 12 shows the conversions and the selectivities in time for the different catalysts. In Table 5 the yields are presented.

From Fig. 12, it is observed that nitrate conversion and nitrogen selectivity are strongly influenced by the Cu/Zn atomic ratio in 1%Pt/CuZnAl-Y catalysts. The conversion increases with the bulk Cu/Zn ratio until a value of 1, and then it decreases with an increase of the copper content. The activity varies strongly among the catalysts and a simple correlation to the copper content cannot be drawn, suggesting that other factors such as the properties of the

Table 5
Yields achieved by the 1%Pt-supported CuZnAl catalysts with different Cu/Zn atomic ratios (steady state values).

Catalysts	Y_{nitrites} (%)	Y_{ammonium} (%)	Y_{nitrogen} (%)
1%Pt/CuZnAl-2	17.6	1.3	6.1
1%Pt/CuZnAl-1	32.0	2.4	7.6
1%Pt/CuZnAl-0.5	4.1	0.2	2.8

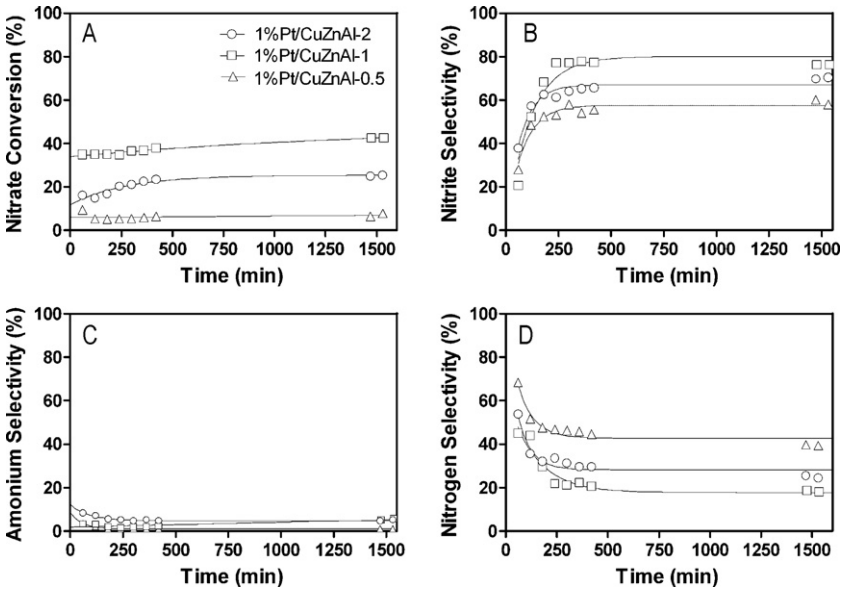

Fig. 12. 1%Pt supported over CuZnAl mixed oxides with different Cu/Zn ratios.

dispersing oxide phase plays an important role (as it was reported by Turco et al. [44] in the OSRM reaction using CuZnAl mixed oxides). The samples exhibit similar surface characteristics: BET surface areas, particle size and morphology (see HRTEM) and Pt dispersion (see XPS) are comparable in all catalysts. As a consequence, the differences in the catalytic activity should be more likely related to differences in the surface composition induced by changing the Cu/Zn atomic ratio during the synthesis of the HT precursors (see Table 4).

The differences in conversion (Fig. 12A) could be attributed to differences in the copper surface atomic composition, because it is generally accepted that metallic copper sites are the active ones to reduce nitrates [18,45]. The low conversion achieved by 1%Pt/CuZnAl-0.5 compared to the other samples, might be explained by the low $Cu/Al_{(XPS)}$ and $Cu/Zn_{(XPS)}$ ratios (see Table 4). It means that there is an Al enrichment of the surface and copper is not available to react with the nitrates.

Usually, catalysts reported in the literature for the nitrate reduction reaction in water contain around 0.25–2 wt% Cu [30,52], but in the present study the catalysts contained between 20 and 47 wt% relative to the support weight. The copper content was changed drastically between catalysts in order to obtain significant differences in the interactions of the metals in the support. Also, conversions are lower than the reported for other Pt-Cu catalysts tested at similar reaction conditions [30] with low copper content, but this could be explained because all the copper is not on the surface like in copper impregnated materials. This can be related to: (i) the deficient formation of Cu-Pt bimetallic sites (that presented higher nitrate removal rate than copper monometallic sites [21]), and (ii) to the insufficient close contact between Pt and Cu on the surface of the catalysts [21] (as it is observed by HRTEM analyses), thus all active sites to remove nitrates are not regenerated.

Catalyst 1%Pt/CuZnAl-0.5 presents the highest nitrogen selectivity (39%) (Fig. 12D), but in view of the differences in conversion, it is more adequate to consider the nitrogen yield than the nitrogen selectivity for comparative purposes (see Table 5). In terms of nitrogen yield the best catalyst is 1%Pt/CuZnAl-1.

The nitrite yield increases while conversion increases (Fig. 12B), indicating that the nitrate reduction rate of reaction is faster than the nitrite reduction rate. This behavior was observed previously by Wang et al. [26]. High nitrite selectivity (i.e. low nitrogen yield) was achieved in all cases, this could be related to the fact that Pt is preferentially supported on Zn- and Al- containing phases than on CuO or Cu(0) phases, as it was observed by HRTEM. According to previous studies [18], nitrates are reduced on metallic copper to produce nitrites, involving a redox reaction where copper is oxidized. Besides, Pt plays two important roles in the reaction: (1) to regenerate the copper oxide by reduction to metallic copper, and (2) to reduce the intermediate product (nitrite), to nitrogen. Also, it was reported that Pt-Cu sites can reduce nitrite to nitrogen in a higher rate compared to the Pt monometallic sites [21]. Consequently, because Pt is not preferentially in close contact with copper sites on the surface of these catalysts, it seems that the nitrite generated does not enter in contact enough time with Pt sites or Pt-Cu bimetallic sites to be reduced to nitrogen or ammonium [45]. In this case, Pt sites in the catalysts are close enough to regenerate copper by hydrogen spillover, but not enough to reduce all the nitrites, confirming that the interaction between copper and platinum is of major importance to reduce nitrates and nitrites as mentioned by Epron et al. [21] and Sá et al. [23,44]. Nevertheless, the influence of the interaction between Pt-Cu in the nitrate hydrogenation reaction is still not clear; as a consequence a more detailed study is being performed currently.

Ammonium concentrations up to 1 ppm were detected (Fig. 12C), these concentrations are significantly lower compared to the reported by Palomares et al. [29] using 5%Pd/CuMgAl catalysts. The low ammonium formation in all catalysts is due to the low amount of Pt. Besides, the hydrogenation ability of Pt is affected by the high content of copper in the supports [45], avoiding over-reduction of nitrites.

The samples do not present partial reconstruction of the mixed oxide phase into HT structure after the catalytic tests, as it was observed by Palomares et al. in [29] using Pd supported on CuMgAl calcined HT. This is due to the insertion of Zn instead of Mg in the HT structure and to the significant difference in copper content. The mechanism proposed in [29] could not be verified in this case using HT-type materials due to their different rehydration properties.

3.2.2. *Incidence of the Pt metal loading*

Considering the high nitrite selectivities observed, different Pt metal loadings were supported on the CuZnAl-1 sample (the support that presented the highest nitrogen yield and best conversion reported in Table 5), to obtain more Pt particles available on the surface to reduce the excess of nitrites. Fig. 13 presents the conver-

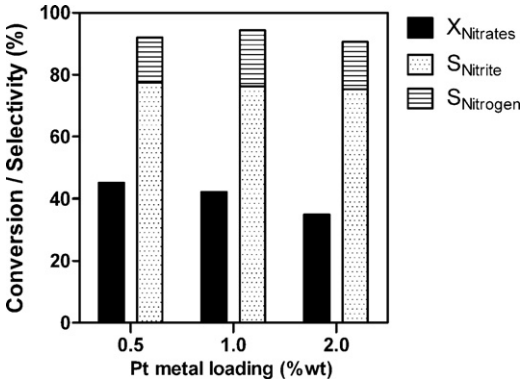

Fig. 13. Study of the incidence of the metal loading over Pt/CuZnAl-1 samples.

Table 6
Yields of Pt/CuZnAl catalysts with different Pt metal loading.

Catalysts	$Y_{nitrites}$ (%)	$Y_{ammonium}$ (%)	$Y_{nitrogen}$ (%)
0.5%Pt/CuZnAl-1	34.8	3.6	6.6
1%Pt/CuZnAl-1	32.0	2.4	7.6
2%Pt/CuZnAl-1	26.4	3.3	5.4

sion and selectivities obtained for catalysts with 0.5%, 1%, and 2% Pt. The ammonium, nitrite and nitrogen yields in steady state are presented in Table 6.

From Fig. 13 it is observed that similar conversions and selectivities are obtained in a range between 0.5 and 2 wt% Pt, and ammonium selectivities around 10% are achieved. No significant improvements in the nitrogen yield (see Table 6) are observed, and it seems that the Cu–Pt interaction does not change with the Pt metal loading in this range. A higher Pt content and other synthesis method should be tried in order to cause a different interaction between the metals on the surface as it was previously reported [52]. Also, it would be interesting to co-precipitate Pt precursor during the HT synthesis to favor Pt–Cu interaction.

3.2.3. Support catalytic tests

To complement the study, the catalytic activities of the CuZnAl-Y supports were tested as reference materials (monometallic catalysts). The samples were pretreated at 300 °C in hydrogen flow, and then tested in the same conditions described for catalytic tests. The results are presented in Fig. 14.

CuZnAl-Y are practically inactive for the nitrate reduction reaction, indicating that nitrate can be reduced on copper monometallic sites, but the degradation rate is very low in agreement with previous investigations [31,53]. It is generally accepted that monometallic sites are inactive for nitrate reduction, and the results confirm that the presence of a noble metal (like Pt) is necessary to enhance the catalytic activity. No ammonium formation or desorption is observed, and up to 0.5 ppm of nitrites are detected due to the catalytic reduction of nitrates.

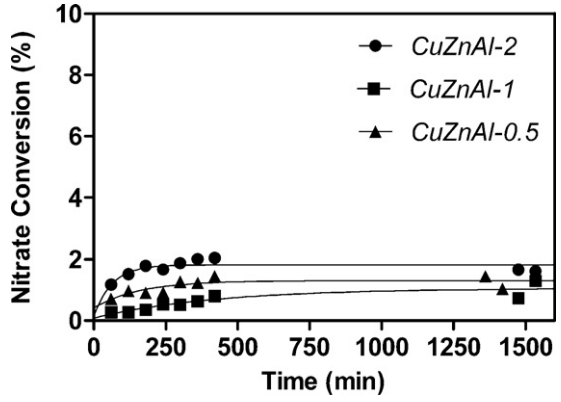

Fig. 14. Conversion of CuZnAl supports with different Cu/Zn atomic ratios.

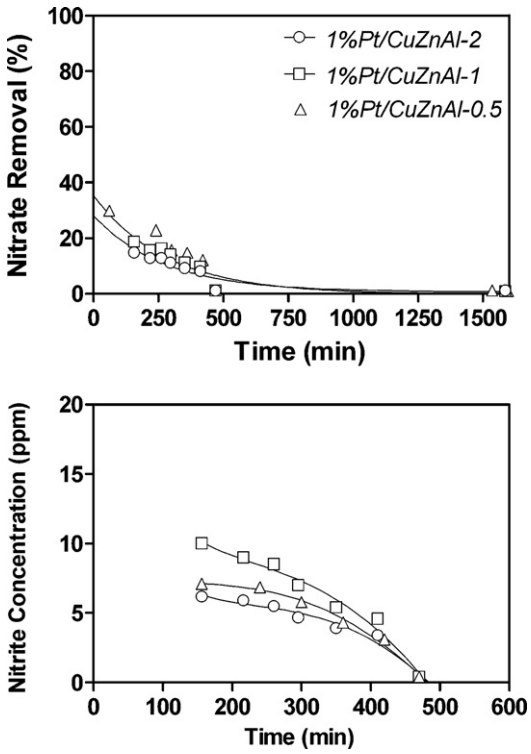

Fig. 15. Adsorption tests of Pt-impregnated CuZnAl mixed oxides with different Cu/Zn atomic ratio.

3.2.4. Catalysts stability

It is important to evaluate the stability of the catalysts in order to determine the leaching of copper, thus after the reaction the copper concentration in the treated water was analyzed by atomic absorption. The copper concentration was less than 15 ppb in all cases and the values were under the potable water limitations (2 ppm) of the European Union [54].

3.3. Adsorption tests

Adsorption test for the 1%Pt/CuZnAl-Y catalysts were performed in the same conditions as the catalytic tests, but no hydrogen was fed to the reactor while the nitrate solution was pumped. The materials were previously reduced under hydrogen flow at 300 °C before the tests. The results are presented in Fig. 15.

It is observed that the nitrate removal rate decreases rapidly in time when no hydrogen was fed to the reactor; this is due to surface oxidation of copper showing that hydrogen is necessary as reducing agent to regenerate copper sites [18,21]. Ammonium concentrations under the detection limits (after 500 min) and nitrite concentration around 0.4 ppm were detected. Consequently, after 1000 min the contribution of nitrate removal due to adsorption can be neglected in the catalytic tests. The same tendency was observed in the tests performed with CuZnAl-Y supports, for which no ammonium was detected.

4. Conclusions

Pt-supported CuZnAl calcined HT materials, with different Cu/Zn atomic ratios (0.5, 1 and 2) and a (Cu + Zn)/Al atomic ratio of 3, were synthesized and characterized by different techniques. The catalysts were tested in the catalytic reduction of nitrates in water, and demonstrated to be active and stable in this reaction. The Cu/Zn atomic ratio in the active support (CuZnAl-Y) has a strong influence in the nitrate conversion and in the nitrogen selectivity, indicating that the interaction of the different components in the support plays an important role in the catalytic activity. The highest conversion and nitrogen yield were obtained with 1%Pt/CuZnAl-1 catalysts. A simple correlation of the catalytic activity with the copper content was not observed. The Pt content does not influence significantly the selectivity or conversion in the range studied (0.5–2 wt%), due to the low Pt/Cu ratio. A further optimization of the system should be performed in order to improve the nitrogen selectivity.

The CuZnAl calcined HT as supports are practically inactive for nitrate reduction and Pt is necessary to enhance the activity.

Acknowledgments

Authors are grateful to Universitat Rovira i Virgili, the Spanish Ministry of Science and Innovation (Ramon y Cajal Program funding S.C.) and Project 2008ITT-CTP-00111, for funds received to carry out this investigation; with the support of the "Comisionado para Universidades e Investigación del Departamento de Innovación, Universidades y Empresa de la Generalitat de Catalunya", and the European Social Fund. F. Medina and J. Llorca acknowledge Generalitat de Catalunya for ICREA ACADEMIA award.

References

[1] L.W. Canter, Nitrates in Groundwater, CRC Press, Boca Raton, 1996.
[2] European Communities (Drinking Water) (No. 2), Regulations 2007, Statutory instruments.
[3] Health Canada, Guidelines for Canadian Drinking Water Quality, 6th ed., Ministry of Health, Ottawa, 1996.
[4] K.M. Hiscock, J.W. Lloyd, D.N. Lerner, Water Res. 25 (1991) 1099.
[5] A. Kapoor, T. Viraraghavan, A. Fellow, J. Environ. Eng. (Reston, VA, US) 123 (1997) 371.
[6] M. Shrimali, K.P. Singh, Environ. Pollut. 112 (2001) 351.
[7] N. Barrabés, A. Dafinov, F. Medina, J.E. Sueiras, Catal. Today 149 (2010) 341.
[8] G. Centi, S. Perathoner, Appl. Catal. B 41 (2003) 15.
[9] J.N. Cevaal, W.B. Suratt, J.E. Burke, Desalination 103 (1995) 101.
[10] J.B. de Heredia, J.R. Dominguez, Y. Cano, I. Jimenez, Appl. Surf. Sci. 252 (2006) 6031.
[11] M.I.M. Soares, Water Air Soil Pollut. 123 (2000) 183.
[12] J.P. van der Hoek, A. Klapwijk, Water Res. 21 (1987) 989.
[13] U. Prusse, M. Hahnlein, J. Daum, K.-D. Vorlop, Catal. Today 55 (2000) 79.
[14] K.-D. Vorlop, T. Tacke, Chem. Ing. Tech. 61 (1989) 836.
[15] F.A. Marchesini, S. Irusta, C. Querini, E. Miro, Catal. Commun. 9 (2008) 1021.
[16] A.J. Lecloux, Catal. Today 53 (1999) 23.
[17] A. Pintar, J. Batista, Catal. Today 53 (1999) 35.
[18] U. Prüsse, K.-D. Vorlop, J. Mol. Catal. A: Chem. 173 (2001) 313.
[19] Y.-X. Chen, Y. Zhang, G.-H. Chen, Water Res. 37 (2003) 2489.
[20] Y. Wang, J. Qu, H. Liu, J. Mol. Catal. A: Chem. 272 (2007) 31.
[21] F. Epron, F. Gauthard, C. Pinéda, J. Barbier, J. Catal. 198 (2001) 309.
[22] U. Prusse, S. Horold, K.D. Vorlop, Chem. Ing Tech. 69 (1997) 93.
[23] J. Sá, H. Vinek, Appl. Catal. B. 57 (2005) 247.
[24] A. Garron, K. Lazar, F. Epron, Appl. Catal. B. 59 (2005) 57.
[25] A.E. Palomares, C. Franch, A. Corma, Catal. Today 149 (2010) 348.
[26] Y. Wang, J. Qu, H. Liu, R. Wu, Chin. Sci. Bull. 51 (2006) 1431.
[27] F. Gauthard, F. Epron, J. Barbier, J. Catal. 220 (2003) 182.
[28] A.E. Palomares, J.G. Prato, F. Márquez, A. Corma, Appl. Catal. B. 41 (2003) 3.
[29] A.E. Palomares, J.G. Prato, F. Rey, A. Corma, J. Catal. 221 (2004) 62.
[30] N. Barrabés, J. Just, A. Dafinov, F. Medina, J.L.G. Fierro, J.E. Sueiras, P. Salagre, Y. Cesteros, Appl. Catal. B. 62 (2006) 77.
[31] O.S.G.P. Soares, J.J.M. Órfão, M.F.R. Pereira, Catal. Lett. 126 (2008) 253.
[32] I. Witonska, S. Karski, N. Krawczyk, Pol. J. Chem. 82 (2008) 171.
[33] J. Sá, T. Berger, K. Föttinger, A. Riss, J.A. Anderson, H. Vinek, J. Catal. 234 (2005) 282.
[34] W. Gao, J. Chen, X. Guan, R. Jin, F. Zhang, N. Guan, Catal. Today 93–95 (2004) 333.
[35] D. Gasparovicová, M. Králik, M. Hronec, Z. Vallusová, H. Vinek, B. Corain, J. Mol. Catal. A: Chem. 264 (2007) 93.
[36] D. Wan, H. Liu, X. Zhao, J. Qu, S. Xiao, Y. Hou, J. Colloid Interface Sci. 332 (2009) 151.
[37] Y. Wang, J. Qu, H. Liu, C. Hu, Catal. Today 126 (2007) 476.
[38] A. Aristizábal, N. Barrabés, S. Contreras, M. Kolafa, D. Tichit, F. Medina, J. Sueiras, Phys. Procedia 8 (2010) 44.
[39] F. Cavani, F. Trifirò, A. Vaccari, Catal. Today 11 (1991) 173.
[40] Y. Matatov-Meytal, V. Barelko, I. Yuranov, M. Sheintuch, Appl. Catal. B 27 (2000) 127.
[41] D. Debecker, E. Gaigneaux, G. Busca, Chem. Eur. J. 15 (2009) 3920.
[42] T. Shishido, M. Yamamoto, D. Li, Y. Tian, H. Morioka, M. Honda, T. Sano, K. Takehira, Appl. Catal. A 303 (2006) 62.
[43] S. Murcia-Mascarós, R.M. Navarro, L. Gómez-Sainero, U. Costantino, M. Nocchetti, J.L.G. Fierro, J. Catal. 198 (2001) 338.
[44] M. Turco, G. Bagnasco, C. Cammarano, P. Senese, U. Costantino, M. Sisani, Appl. Catal. B 77 (2007) 46.
[45] Y. Yoshinaga, T. Akita, I. Mikami, T. Okuhara, J. Catal. 207 (2002) 37.
[46] C. Busetto, G. Del Piero, G. Manara, F. Trifirò, A. Vaccari, J. Catal. 85 (1984) 260.
[47] M. Behrens, I. Kasatkin, S. Kuľhl, G. Weinberg, Chem. Mater. 22 (2009) 386.
[48] J.P. Breen, J.R.H. Ross, Catal. Today 51 (1999) 521.
[49] Z. Tang, D. Geng, G. Lu, Mater. Lett. 59 (2005) 1567.
[50] M. Turco, G. Bagnasco, U. Costantino, F. Marmottini, T. Montanari, G. Ramis, G. Busca, J. Catal. 228 (2004) 43.
[51] N.W. Hurst, S.J. Gentry, A. Jones, B.D. McNicol, Catal. Rev. - Sci. Eng. 24 (1982) 233.
[52] F. Epron, F. Gauthard, J. Barbier, J. Catal. 206 (2002) 363.
[53] K.D. Vorlop, U. Prusse, Catalytic Science Series, vol. 1, Imperial College Press, 1999, p. 369.
[54] EEC—European Economic Community, The Drinking Water Directive (DWD) Council Directive 98/83/EC, concerns the quality of water intended for human consumption., 1998, p. Annexe I. Part B.